Int. J. Heat Mass Transfer. Vol. 35, No. 2, pp. 457–467, 1992
Printed in Great Britain

0017-9310/92 $5.00 + 0.00

A numerical method for phase-change problems with convection and diffusion

CHARN-JUNG KIM and MASSOUD KAVIANY
Department of Mechanical Engineering and Applied Mechanics, The University of Michigan, Ann Arbor, MI 48109, U.S.A.

(*Received* 26 *September* 1990 *and in final form* 20 *February* 1991)

Abstract—An existing finite-difference formulation, which uses immobilization of the moving interface while preserving the conservative form of the equations, is extended here to include convection and volume change. In this two-dimensional treatment, the physical boundaries are allowed to move in both coordinate directions. This is done by using a novel technique that discretizes the pseudo-velocities (arising from the immobilization) according to the geometrical relation associated with the moving control-volumes. As a result, the pseudo-velocity fields independently satisfy the mass continuity. This makes the present numerical method suitable for both diffusion- and convection/diffusion-controlled moving boundary problems. In the solution of the momentum equations, the physical covariant velocity components are selected as the dependent variables and the SIMPLER algorithm is employed for the coupling between the continuity and the momentum equations. The method is applicable to problems with multiple, moving interfaces. As an illustrative example, melting in a two-dimensional cavity is considered. The predictions are then compared with the available experimental results and good agreements are found.

1. INTRODUCTION

ONE OF THE finite-difference methods introduced recently for two-dimensional moving interface problems [1] uses a coordinate transformation that preserves the conservative form of the governing equations. The development in ref. [1] focuses on diffusion only and, although not an inherent limitation, it allows for the movement of physical domain boundaries in a single coordinate direction. In this study, we extend the treatment to include convection and volume change, and to allow for the movement of the boundaries in both coordinate directions.

A variety of numerical methods are available for treatment of convection/diffusion phase-change problems; however, they suffer in generality of application and in accuracy. Sparrow *et al.* [2] give the first numerical analysis of phase-change problems accounting for natural convection in the melt. In their work, the slope of the interface is neglected and temporal interpolation of the known fields (velocity and temperature) is required to update the unknown fields. In the numerical study of Benard *et al.* [3], natural convection in the melt is coupled with heat conduction in the solid phase. The non-orthogonal terms resulting from the use of a coordinate transformation are neglected. Steady state is assumed in the liquid phase while the transient terms are included in the solid phase, i.e. two different solution methods are applied. Lacroix [4] uses the stream function–vorticity formulation and includes the transient and the non-orthogonal terms in the transformed equations expressed in non-conservative forms. The accuracy of this method is not examined by, for example, applying the conventional test on the diffusion-controlled phase-change problems for which analytical solutions are available. In general, the drawbacks of these numerical methods (and other available methods) are that the transformed equations are expressed in non-conservative forms and that the interface conditions are treated separately from the transformed equations. Therefore, their formulations weakly satisfy the conservation principles. Also, the density difference between phases, which can be significant in some cases, is not included.

In order to overcome the shortcomings mentioned, we employ a general transformed equation which preserves the conservative forms of the original governing equations. Also, we derive the interface conditions directly from the continuity of the fluxes in the transformed equation. As a result, the present numerical formulation is consistent with the well-established solution methodology for problems with fixed boundaries (e.g. Patankar [5]). In deriving the discretization equations, the moving control-volumes in the physical coordinate as well as the stationary control-volumes in the transformed coordinate are used. The pseudo-velocities arising from the immobilization of the moving boundaries are discretized in accordance with the geometrical relation associated with the moving control-volumes. Then, the pseudo-velocity fields satisfy the continuity equation independent of the physical velocity fields. Therefore, both diffusion- and convection/diffusion-controlled moving interface problems can be solved with a unified approach. Moreover, a multiple number of moving boundaries can be easily treated. For the computation of the fluid motion, an efficient calculation procedure recently proposed by Karki and Patankar [6] is adopted and modified accounting for the moving boundaries.

NOMENCLATURE

A	area term or function
a	coefficient in finite-difference equations
b	source term in finite-difference equations
c	specific heat capacity [J kg^{-1} K^{-1}]
c_r	ratio c_2/c_1
D	diffusion conductance
F	flow term
$\hat{G}_1$	mass flow rate across the interface $\hat{x}_1$
H	initial height of the material [m]
h	specific enthalpy [J kg^{-1}]
h_{sf}	latent heat of liquid/solid phase change [J kg^{-1}]
h_ξ, h_η	geometric factors
J	Jacobian
k	thermal conductivity [W m^{-1} K^{-1}]
k_r	ratio k_2/k_1
L	thickness of the liquid overflow region [m]
M, N	geometric factors
P	pressure [Pa]
P^*	dimensionless pressure, $PH^2/\rho_1\nu^2$
Pr	Prandtl number, ν/α_1
Ra	Rayleigh number, $g\beta(\hat{T}_0-\hat{T}_1)H^3/(\alpha_1\nu)$
S	source term
Ste	Stefan number, $c_1(\hat{T}_0-\hat{T}_1)/h_{sf}$
$T_1(T_2)$	temperature distribution in the liquid (solid) phase [K]
$\hat{T}_0(\hat{T}_2)$	temperature at the hot (cold) vertical wall [K]
$\hat{T}_1$	melting temperature of the material [K]
T_i^*	dimensionless temperature, $(T_i-\hat{T}_1)/(\hat{T}_0-\hat{T}_1)$
$\hat{T}_i^*$	dimensionless temperature at the boundary $\hat{x}_i$, $(\hat{T}_i-\hat{T}_1)/(\hat{T}_0-\hat{T}_1)$
t	time [s]
t^*	dimensionless time$(=\nu t/H^2)$
Δt	time increment [s]
U, V	relative, contravariant velocities
u, v	Cartesian velocities [m s^{-1}]
u^*, v^*	dimensionless velocities, uH/ν, vH/ν
u_η, u_ξ	covariant velocity components [m s^{-1}]
u_{out}	velocity at the outlet [m s^{-1}]
ΔV	finite-volume element
v_{top}	vertical velocity of the free surface [m s^{-1}]
W	width [m]
X_t, Y_t	contravariant pseudo-velocities
x, y, z	spatial coordinates [m]
x_t, y_t	pseudo-velocities [m s^{-1}]
x^*, y^*	dimensionless coordinates, x/H, y/H
$\hat{x}_i$	position of the boundary with $i = 0, 1, 2$, [m].

Greek symbols

α	thermal diffusivity [m^2 s^{-1}]
α_ξ, α_η	geometric factors
β_ξ, β_η	geometric factors
Γ	effective diffusion coefficient
η	transformed coordinate
λ	geometric factor
ν	kinematic viscosity [m^2 s^{-1}]
ξ	transformed coordinate
ρ	density [kg m^{-3}]
ρ_r	ratio ρ_2/ρ_1
ϕ	general dependent variable
Ω	integrated non-orthogonal term.

Superscripts

0	known quantities at the old time
*	dimensionless quantities
^	quantities at the boundary.

Subscripts

1	liquid
2	solid
e, w, n, s	east, west, north, and south control-volume faces
E, W, N, S	east, west, north, and south grid points
MB	moving-boundary term
NO	non-orthogonal term
nb	neighbor
P	grid point under consideration.

As an application of the present numerical method, melting in a two-dimensional cavity driven by the coupling of heat conduction in the solid phase and natural convection in the liquid phase is considered. For this example, the results of an experiment are available [3]. In the numerical analysis, the density difference between phases and the overflow of the liquid are also included using a simple model.

2. NUMERICAL FORMULATION

2.1. *Governing equations*

The conservation equation for a general dependent variable ϕ, in two-dimensional Cartesian coordinates, is expressed as

$$\frac{\partial}{\partial t}(\rho\phi)+\frac{\partial}{\partial x}\left(\rho u\phi-\Gamma\frac{\partial\phi}{\partial x}\right)+\frac{\partial}{\partial y}\left(\rho v\phi-\Gamma\frac{\partial\phi}{\partial y}\right)=S(x,y) \quad (1)$$

where Γ is the effective diffusion coefficient and $S(x, y)$ is the source term corresponding to ϕ. The density ρ is assumed to be constant within each physical domain of interest. When the boundaries of the physical domain move with time, it is convenient to introduce a general curvilinear coordinate system

$$x = x(\xi,\eta,t), \quad y = y(\xi,\eta,t) \quad (2)$$

so that the moving boundaries are immobilized in the

dimensionless† (ξ, η) coordinate for all times. Then, transformation of equation (1), using equation (2), gives

$$\frac{\partial}{\partial t}(J\rho\phi)+\frac{\partial}{\partial \xi}\left(\rho U\phi-\frac{\alpha_\xi \Gamma}{h_\xi}\frac{\partial \phi}{\partial \xi}\right)+\frac{\partial}{\partial \eta}\left(\rho V\phi-\frac{\alpha_\eta \Gamma}{h_\eta}\frac{\partial \phi}{\partial \eta}\right)=JS(\xi,\eta)-\frac{\partial}{\partial \xi}\left(\frac{\beta_\xi \Gamma}{h_\eta}\frac{\partial \phi}{\partial \eta}\right)-\frac{\partial}{\partial \eta}\left(\frac{\beta_\eta \Gamma}{h_\xi}\frac{\partial \phi}{\partial \xi}\right) \quad (3)$$

where

$$U = y_\eta(u-x_t)-x_\eta(v-y_t)$$
$$V = x_\xi(v-y_t)-y_\xi(u-x_t)$$
$$\alpha_\xi = h_\xi h_\eta^2/J, \quad \alpha_\eta = h_\eta h_\xi^2/J$$
$$\beta_\xi = \lambda h_\eta/J, \quad \beta_\eta = \lambda h_\xi/J$$
$$h_\xi = (x_\xi^2+y_\xi^2)^{1/2}, \quad h_\eta = (x_\eta^2+y_\eta^2)^{1/2}$$
$$\lambda = x_\xi x_\eta + y_\xi y_\eta, \quad J = x_\xi y_\eta - y_\xi x_\eta.$$

Here, x_t, x_ξ, x_η, y_t, y_ξ and y_η denote partial derivatives. The terms U and V represent the relative, contravariant velocity components normal to the constant ξ- and η-coordinate lines, respectively; and $S(\xi, \eta)$ is the source term in the transformed coordinate.

2.2. *Grid system*

The grid system is a staggered-grid with the scalars at the center of the control-volume and the velocity components at its faces [5]. Thus, at a given time, the physical domain of interest is divided into a set of non-overlapping, quadrilateral control-volumes. Figure 1 shows the control-volume surrounding the main grid point P and shows the designation used for the neighboring nodes. In constructing the control-volumes in the physical coordinate, the positions of the corner points of the control-volumes are deployed first in accordance with the predetermined control-volumes in the transformed coordinate. Then, all the corner points are connected by straight lines assuming piecewise linear transformations between the corners. The main grid point for the scalars is located at the geometrical center of each control-volume. The positions locating the velocity components are placed midway between the corner points.

Figure 2 illustrates a typical moving control-volume in the physical coordinate, where the quadrangle $A^0B^0C^0D^0$ is the *old* control-volume at time t^0 and the quadrangle $ABCD$ is the *new* control-volume after an elapsed time of Δt. These two moving control-volumes correspond to a single control-volume that is stationary in the transformed coordinate. The

† For example, even when $x = \xi$ and $y = \eta$, these relations can be interpreted as x = (unit length) $\times \xi$, etc. Subsequently, the product of velocity and length will be called velocity for the sake of brevity.

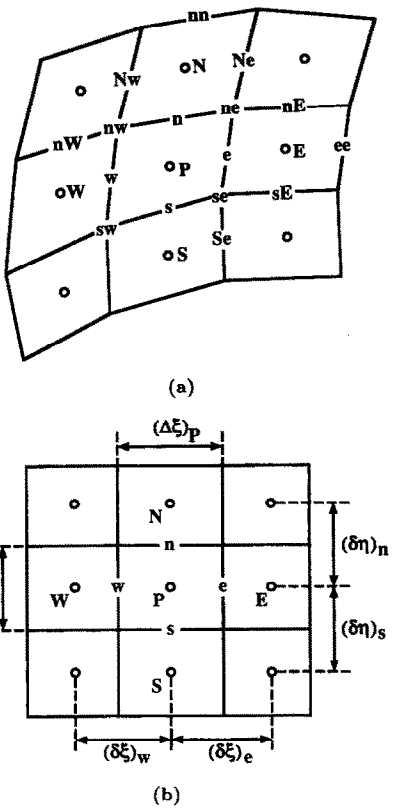

FIG. 1. Configuration of the control-volumes in the physical coordinate (a) and in the transformed coordinate (b).

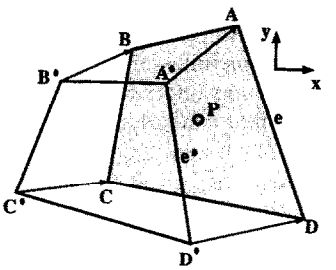

FIG. 2. A schematic of the moving control-volume in the physical coordinate.

following *area rule* holds between the two moving control-volumes shown in Fig. 2:

$$m(ABCD)-m(A^0B^0C^0D^0)-m(AA^0D^0D)+m(BB^0C^0C)-m(BB^0A^0A)+m(CC^0D^0D)=0 \quad (4)$$

where the absolute value of $m(ABCD)$ denotes the area enclosed by the quadrangle $ABCD$ (positive if $ABCD$ rotates counter-clockwise and negative otherwise).

2.3. *Continuity equation*

The discretized continuity equation (for $\phi = 1$ and $S = 0$) is obtained by integrating equation (3) over

the stationary control-volume in the transformed coordinate. This gives

$$\frac{\rho_P(\Delta V)_P-\rho_P^0(\Delta V)_P^0}{\Delta t}+F_e-F_w+F_n-F_s=0 \quad (5)$$

where $(\Delta V)_P=J_P(\Delta\xi)_P(\Delta\eta)_P$ is the area of the quadrangle $ABCD$ and $(\Delta V)_P^0$ is that of the quadrangle $A^0B^0C^0D^0$. The discretized representation of F values requires a special treatment due to the existence of pseudo-velocities. Consider first the cases in which the continuity equation is trivially satisfied (i.e. $\rho=$ constant and $u=v=0$) as occurring in diffusion-controlled moving-boundary problems. It is then convenient to introduce X_t and Y_t such that

$$X_t=y_\eta x_t-x_\eta y_t, \quad Y_t=x_\xi y_t-y_\xi x_t \quad (6)$$

which represent the contravariant pseudo-velocities normal to the constant ξ- and η-coordinate lines, respectively. For this special case, the discretization of X_t and Y_t should be made in such a way that equation (5) becomes identically zero. This can be done by evaluating all the terms in equation (5) at the same time $(t^0+\Delta t/2)$, i.e. interpreting an implicit-difference as a central-difference representation with respect to time $(t^0+\Delta t/2)$ [7]. Therefore, $X_{t,e}$ is discretized as

$$X_{t,e}=y_{\eta,e}^{(1/2)}x_{t,e}-x_{\eta,e}^{(1/2)}y_{t,e}$$
$$=\frac{1}{2\Delta t}\{(y_{\eta,e}+y_{\eta,e}^0)(x_e-x_e^0)-(x_{\eta,e}+x_{\eta,e}^0)(y_e-y_e^0)\} \quad (7)$$

which makes the quantity $X_{t,e}(\Delta\eta)_P(\Delta t)$ equal to the positive (or negative) value of the area swept by line AD during the time interval Δt, i.e. $m(AA^0D^0D)$ in Fig. 2. Other pseudo-velocity terms $X_{t,w}$, $Y_{t,n}$ and $Y_{t,s}$ are also discretized similarly. Note that the present discretization of the pseudo-velocities simply represents the area rule given in equation (4), thus enabling equation (5) to become identically zero. The final expressions for F values will be shown later.

2.4. *General conservation equation*

In this section, the discretization procedure for a general dependent variable ϕ other than the velocity components is described. The integration of the transformed equation (3), with the aid of the discretized continuity equation (5), gives

$$a_P\phi_P=a_E\phi_E+a_W\phi_W+a_N\phi_N+a_S\phi_S+b+b_{NO} \quad (8)$$

with

$$a_P=a_E+a_W+a_N+a_S+a_P^0-S_P(\Delta V)_P$$
$$a_P^0=\rho_P^0(\Delta V)_P^0/\Delta t$$
$$a_E=D_eA(F_e/D_e)+\max\{0,-F_e\}$$
$$a_W=D_wA(F_w/D_w)+\max\{0,F_w\}$$
$$a_N=D_nA(F_n/D_n)+\max\{0,-F_n\}$$
$$a_S=D_sA(F_s/D_s)+\max\{0,F_s\}$$
$$b=a_P^0\phi_P^0+S_C(\Delta V)_P$$
$$b_{NO}=-\Omega_e+\Omega_w-\Omega_n+\Omega_s$$
$$D_e=\frac{\alpha_{\xi,e}\Gamma_e(\Delta\eta)_P}{h_{\xi,e}(\delta\xi)_e}, \quad D_w=\frac{\alpha_{\xi,w}\Gamma_w(\Delta\eta)_P}{h_{\xi,w}(\delta\xi)_w}$$
$$D_n=\frac{\alpha_{\eta,n}\Gamma_n(\Delta\xi)_P}{h_{\eta,n}(\delta\eta)_n}, \quad D_s=\frac{\alpha_{\eta,s}\Gamma_s(\Delta\xi)_P}{h_{\eta,s}(\delta\eta)_s}$$

where S_P and S_C arise from the linearized source terms and the function $A(x)$ used here is that of the power-law scheme [5]:

$$A(x)=\max\{0,(1-0.1|x|)^5\}. \quad (9)$$

The term b_{NO} arises from the non-orthogonality of the coordinate system in the physical plane [6]. To obtain the five-point formulation, b_{NO} is treated as a source term and is evaluated explicitly using a piecewise linear profile for ϕ [6], e.g.

$$\Omega_e=\frac{\beta_{\xi,e}\Gamma_e}{h_{\eta,e}}(\phi_{ne}-\phi_{se}). \quad (10)$$

The above set of discretization equations is very similar to those in ref. [5], and the same solution procedure explained there can be applied, but with special care given to the evaluation of a_P^0 and F values.

2.5. *Momentum equations*

If the transformed equation (3) is written for the Cartesian velocities, u and v, as the dependent variables in the momentum equation, these variables can be treated as scalars because their directions do not change [8]. Therefore, the discretization procedure outlined before can be used with the associated source terms. Now, referring to Fig. 3, the discretization equations for the ξ- and η-momentum equations, with u and v as the dependent variables, are (diffusion conductances and flow terms are identical except for the source terms [6])

$$a_eu_e=\sum a_{nb}u_{nb}+a_e^0u_e^0+b_u$$
$$a_ev_e=\sum a_{nb}v_{nb}+a_e^0v_e^0+b_v \quad (11)$$

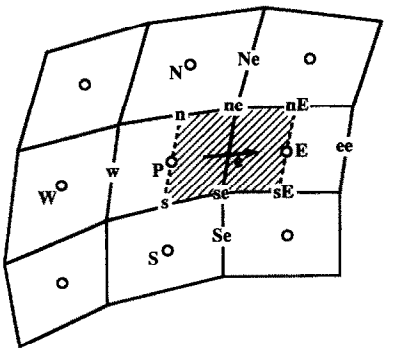

FIG. 3. Control-volumes for the discretization of the velocity component $u_{\xi,e}$.

where nb denotes all the neighboring points (ee, w, Ne and Se) and the source terms b_u and b_v are properly evaluated.

The physical covariant velocity components u_ξ and u_η, the directions of which are along the coordinate lines, are related to u and v as

$$u_\xi = (x_\xi u + y_\xi v)/h_\xi, \quad u_\eta = (x_\eta u + y_\eta v)/h_\eta \quad (12)$$

and the motivation for the use of these velocities is discussed in ref. [8]. The discretization equation for the covariant velocity component $u_{\xi,e}$ is obtained, as suggested in ref. [6], by algebraically combining the discretization equations for u and v in equation (11). The final discretization equation for $u_{\xi,e}$ becomes

$$a_e u_{\xi,e} = \sum a_{nb} u_{\xi,nb} + a_e^0 u_{\xi,e}^0 + b_{\xi,MB} + b_{\xi,NO} + A_e(P_P - P_E) + S_{\xi,e} \quad (13)$$

where

$$b_{\xi,MB} = a_e^0(M_\xi^0 u_{\xi,e}^0 + M_\eta^0 u_{\eta,e}^0)$$

$$b_{\xi,NO} = \sum a_{nb}(u'_\xi - u_\xi)_{nb} - \Omega_{\xi,E} + \Omega_{\xi,P} - \Omega_{\xi,ne} + \Omega_{\xi,se}$$

$$u'_\xi - u_\xi = M_\xi u_\xi + M_\eta u_\eta, \quad A_e = \frac{(\Delta V)_e}{h_{\xi,e}(\delta\xi)_e}$$

and $S_{\xi,e}$ is the discretized source term excluding the pressure gradient. The expressions for M_ξ^0, M_η^0, M_ξ and M_η are given in the Appendix. The velocity u'_ξ is interpreted as the neighboring velocity component parallel to $u_{\xi,e}$ [6, 8]. The source term $b_{\xi,MB}$ arises from the time-wise rotation of the velocity-component base-vectors associated with the movement of the control-volume faces. If the control-volumes move parallel to their old positions by pure displacement, then $b_{\xi,MB}$ becomes zero because $M_\xi^0 = M_\eta^0 = 0$. The source term $b_{\xi,NO}$ is determined using the continuity-satisfying velocity fields from the previous iteration [6]. The Ω_ξ terms in $b_{\xi,NO}$ are expressed similarly to equation (10) as

$$\Omega_{\xi,E} = \frac{\beta_{\xi,E}\Gamma_E}{h_{\eta,E}}(u'_{\xi,nE} - u'_{\xi,sE}), \quad \text{etc.} \quad (14)$$

The discretization equation for $u_{\eta,n}$ can be obtained similarly. The final results are

$$a_n u_{\eta,n} = \sum a_{nb} u_{\eta,nb} + a_n^0 u_{\eta,n}^0 + b_{\eta,MB} + b_{\eta,NO} + A_n(P_P - P_N) + S_{\eta,n} \quad (15)$$

where

$$b_{\eta,MB} = a_n^0(N_\xi^0 u_{\xi,n}^0 + N_\eta^0 u_{\eta,n}^0)$$

$$b_{\eta,NO} = \sum a_{nb}(u'_\eta - u_\eta)_{nb} - \Omega_{\eta,ne} + \Omega_{\eta,nw} - \Omega_{\eta,N} + \Omega_{\eta,P}$$

$$u'_\eta - u_\eta = N_\xi u_\xi + N_\eta u_\eta, \quad A_n = \frac{(\Delta V)_n}{h_{\eta,n}(\delta\eta)_n}$$

and Ω_η terms in $b_{\eta,NO}$ are expressed as

$$\Omega_{\eta,ne} = \frac{\beta_{\xi,ne}\Gamma_{ne}}{h_{\eta,ne}}(u'_{\eta,Ne} - u'_{\eta,e}), \quad \text{etc.} \quad (16)$$

The expressions for N_ξ^0, N_η^0, N_ξ and N_η are listed in the Appendix.

In the discretized momentum equations, the velocity components along the control-volume faces (such as $u_{\xi,n}$ and $u_{\eta,e}$) are linearly interpolated from the continuity-satisfying velocity fields obtained in the previous iteration [6]. The solution of the above discretized momentum equations requires the specification of the pressure field. Unless this pressure field is correctly specified, the resulting velocities will not in general satisfy the mass continuity and the pressure correction equations are needed. These equations are obtained from the discretized continuity equation (5) rewritten in terms of u_ξ and u_η. Therefore, U and V are expressed as

$$U = \alpha_\xi u_\xi - \beta_\xi u_\eta - X_t, \quad V = \alpha_\eta u_\eta - \beta_\eta u_\xi - Y_t \quad (17)$$

from which the flow terms F are determined as

$$F_e = \rho_e(\alpha_\xi u_\xi - \beta_\xi u_\eta - X_t)_e(\Delta\eta)_P \quad (18)$$

and so forth. Then, the discretized continuity equation (5) becomes [using $(\Delta\eta)_P = (\Delta\xi)_P = 1$, for brevity]

$$(\rho\alpha_\xi u_\xi)_e - (\rho\alpha_\xi u_\xi)_w + (\rho\alpha_\eta u_\eta)_n - (\rho\alpha_\eta u_\eta)_s = b_{NO} \quad (19)$$

where

$$b_{NO} = (\rho\beta_\xi u_\eta)_e - (\rho\beta_\xi u_\eta)_w + (\rho\beta_\eta u_\xi)_n - (\rho\beta_\eta u_\xi)_s \quad (20)$$

is evaluated using the continuity-satisfying velocity field from the previous iteration [6]. Note that the terms associated with the moving control-volumes (i.e. X_t and Y_t) have disappeared in equation (19) from the assumption of constant density. The SIMPLER algorithm [5] is used to obtain the velocity field by coupling the continuity and the momentum equations. Details of the treatment of the source terms (i.e. $S_{\xi,e}$ and $S_{\eta,n}$), the pressure correction equation, the pressure equation and the overall solution procedure can be found in refs. [6, 8].

3. EXAMPLE PROBLEM

In the above discretization formulation, no particular type of moving boundary was explicitly specified, thus making this treatment of moving boundaries very general. Therefore, the method presented is applicable to problems with a multiple number of moving interfaces. These interfaces can be those between immiscible fluids, between fluids and solids, as well as phase-change interfaces of a single-component substance.

In order to validate the present numerical method, a specific phase-change problem involving natural convection is solved and compared with the available experimental results. The example problem is taken

from the numerical and experimental study of Benard *et al.* [3].

3.1. *Problem description*

The experiment of Benard *et al.* [3] is schematically shown in Fig. 4, where the top and bottom surfaces are insulated. The depth of the enclosure (in the z-direction) is taken sufficiently larger than its height and width, in anticipation that the heat transfer and the fluid flow are two-dimensional. The enclosure is initially filled with the solid phase, leaving an air gap on top to allow for the volume expansion upon melting. The solid is initially at a uniform temperature $\hat{T}_2$ below the melting temperature $\hat{T}_1$. At $t = 0$, the temperature of the left wall ($\hat{x}_0 = 0$) is raised to a value $\hat{T}_0 > \hat{T}_1$, while the right wall ($\hat{x}_2 = W$) is maintained at the initial temperature $\hat{T}_2$. Then, the melting front $\hat{x}_1$ proceeds towards the cold wall $\hat{x}_2$ until a stationary interfacial front is attained. During the melting process, the volume expansion causes the free surface of the liquid to rise and flow over the solid phase, as illustrated schematically in Fig. 4.

3.2. *Numerical analysis*

3.2.1. *Coordinate system.* The transformed coordinate used in the analysis is

$$x = \begin{cases} \xi \hat{x}_1 & \text{for } 0 \leqslant \xi \leqslant 1 \\ \hat{x}_1 + (\xi - 1)(\hat{x}_2 - \hat{x}_1) & \text{for } 1 \leqslant \xi \leqslant 2 \end{cases}$$

$$y = \begin{cases} \eta H & \text{for } 0 \leqslant \eta \leqslant 1 \\ H + (\eta - 1)L & \text{for } 1 \leqslant \eta \leqslant 2 \end{cases} \quad (21)$$

where L is the thickness of the liquid overflow region and is assumed to be a function of time only, i.e. the free surface of the liquid overflow is horizontal at all times. Therefore, there are two moving boundaries in the present analysis; one is the phase-interface and the other is the free surface of the liquid overflow. Figure 4 shows the distribution of the liquid and solid phases, and the position of the interface in both coordinate systems. In the transformed coordinate, the interface is located at $\xi = 1$ for $0 \leqslant \eta \leqslant 1$. The vertical surface through which the liquid flows over the solid phase is named here as an *outlet*, and this outlet is located at $\hat{x}_1 = (\hat{x}_1)_{y=H}$ for $H \leqslant y \leqslant H + L$ in the physical coordinate and at $\xi = 1$ for $1 \leqslant \eta \leqslant 2$ in the transformed coordinate, respectively, as is also shown in Fig. 4. The liquid overflow region above the solid (shaded in Fig. 4) is neglected in the simulation except in the evaluation of L.

3.2.2. *Treatment of the moving interface.* The interfacial mass and energy balances are directly derived from equation (3) considering the continuity of the ξ-component of the fluxes across the interface. The results are

$$(\rho U)_1 = (\rho U)_2 \equiv \hat{G}_1 \quad (22)$$

$$\left(\rho U h - \frac{\alpha_\xi k}{h_\xi}\frac{\partial T}{\partial \xi}\right)_1 = \left(\rho U h - \frac{\alpha_\xi k}{h_\xi}\frac{\partial T}{\partial \xi}\right)_2 \quad (23)$$

where all the quantities are evaluated at the interface and $\hat{G}_1$ is the interfacial mass flux. The discretized form of equation (23) is used to determine $\hat{G}_1$. The use of the power-law scheme requires tedious trial and error, thus here the central-difference scheme is used because it gives an explicit expression for $\hat{G}_1$ [1]. It is then required for consistency that, for the grid points adjacent to the interface, equation (8) be rewritten in central-difference form in the case of $\phi = h$ (or $\phi = T$).

Because $(\hat{u}_\eta)_1 = 0$ at the interface, equation (22) becomes

$$\hat{X}_t = -\frac{\hat{G}_1}{\rho_2} \quad \text{and} \quad (\hat{u}_\xi)_1 = \frac{1}{(\hat{\alpha}_\xi)_1}\left(1 - \frac{\rho_2}{\rho_1}\right)\hat{X}_t \quad (24)$$

the first of which is used to determine the interface position (see ref. [1] for details), and the second serves as the boundary condition for the velocity field in the liquid phase.

3.2.3. *Boundary conditions.* The thickness L is determined from the conservation of the total mass (including the liquid overflow above the solid phase)

$$\rho_1 W(L - L^0) + (\rho_1 - \rho_2)\int_0^1 (\hat{X}_t \Delta t)_{\xi=1}\, d\eta = 0 \quad (25)$$

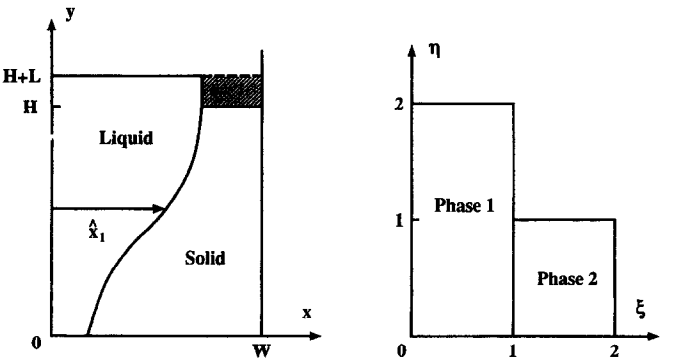

FIG. 4. System geometry for the example problem and the corresponding transformed coordinate system. The shaded area represents the liquid overflow region neglected in the analysis.

Table 1. Variables in the dimensionless governing equations

	ρ^*	ϕ^*	Γ^*	S^*
Liquid	1	1	0	0
		u^*	1	$-\partial P^*/\partial x^*$
		v^*	1	$-\partial P^*/\partial y^* + (Ra/Pr)T_1^*$
		T_1^*	Pr^{-1}	0
Solid	ρ_r	1	0	0
		T_2^*	$(k_r/c_r)\,Pr^{-1}$	0

Table 2. Dimensionless parameters in the example problem

Parameter	Numerical value
W/H	0.389
Pr	52.14
Ste	0.0694
Ra	0.846×10^9
ρ_r	1.051
c_r	0.864
k_r	2.484
$\hat{T}_0^*$	1
$\hat{T}_1^*$	0
$\hat{T}_2^*$	−2.395

where $\hat{X}_t$ is determined explicitly from equation (24). The absolute value of the integrand in equation (25) represents the area swept by the interface during the time interval Δt. Subsequently, all the geometric factors including pseudo-velocities are calculated from the known values of $\hat{x}_1$ and L.

In addition to the interfacial mass and energy balances, the following boundary conditions are used:

$$\text{Left wall:}\quad u = v = 0, \quad T_1 = \hat{T}_0 \tag{26}$$

$$\text{Right wall:}\quad T_2 = \hat{T}_2 \tag{27}$$

$$\text{Bottom wall:}\quad u = v = 0, \quad \frac{\partial T_1}{\partial y} = \frac{\partial T_2}{\partial y} = 0 \tag{28}$$

$$\text{Top wall:}\quad \frac{\partial u}{\partial y} = 0, \quad v = v_{\text{top}}, \quad \frac{\partial T_1}{\partial y} = \frac{\partial T_2}{\partial y} = 0 \tag{29}$$

$$\text{Interface:}\quad u_\xi = (\hat{u}_\xi)_1, \quad u_\eta = 0, \quad T_1 = T_2 = \hat{T}_1 \tag{30}$$

$$\text{Outlet:}\quad u_\xi = u_{\text{out}}, \quad u_\eta = 0, \quad T_1 = \hat{T}_1. \tag{31}$$

The boundary velocity $(\hat{u}_\xi)_1$ is determined explicitly from equation (24). The value of v_{top} is obtained from the kinetic boundary condition at the top free-surface, which can be expressed as $V = 0$ at $\eta = 2$ since no mass can cross this surface. As given in equation (31), the boundary conditions at the outlet are taken to be the same as those at the interface, except for u_ξ. The velocity u_{out} is assumed to be uniform over the outlet and its value can be obtained from the mass balance over the liquid phase alone:

$$\int_0^2 \rho_1 (U + X_t)_{\xi=1}\, d\eta + \int_0^1 \rho_1 (V + Y_t)_{\eta=2}\, d\xi = 0 \tag{32}$$

where $U + X_t$ and $V + Y_t$ denote the physical contravariant velocity components (excluding the pseudo-velocities). The effect of these arbitrarily imposed boundary conditions at the outlet is negligible because the size of the outlet is very small ($L/H < 0.03$ in this example). The major weakness of the simulation rather results from the adiabatic thermal boundary condition at the top surface of the solid phase, and this point will be further discussed later.

3.2.4. *Solution procedure.* The dimensionless governing equations are summarized in Table 1 assuming laminar natural convection in the melt as in ref. [3]. The boundary conditions (26)–(31) are also transformed and discretized. Table 2 lists the numerical values of the dimensionless parameters corresponding to the experiment in ref. [3]. A non-uniformly spaced 22×34 grid is used in the liquid phase and a 22×31 grid in the solid phase; therefore, the liquid overflow region has three grid points in the η-coordinate direction. To initiate the computation, a one-dimensional pure conduction problem is solved until $\hat{x}_1/W = 0.02$, after which laminar natural convection is included. It is found that the subsequent solutions are not sensitive to the value of this prescribed initial thickness. The following procedure is employed for the solution:

(i) Determine the interface position explicitly from equation (24). In doing this, the temperature distributions in the liquid and solid phases are assumed constant during a time interval $(\Delta t)_2$.

(ii) Solve the temperature field in the newly-defined solid phase and go back to step (i) without the solution in the liquid phase. Repeat steps (i) and (ii) for a number of time intervals until $t = t^0 + N(\Delta t)_2$, where $N = 20$ is chosen.

(iii) Solve the heat transfer and the fluid flow in the liquid phase with the time interval $(\Delta t)_1 = N(\Delta t)_2$. Note that, at this stage, the interface positions at both $t = t^0$ and $t = t^0 + (\Delta t)_1$ are necessary to determine the pseudo-velocities in the liquid phase.

(iv) Repeat steps (i)–(iii) until a stationary interface position is attained.

The maximum value of the dimensionless time step $(\Delta t^*)_1$ used in the computation is 0.1, where the dimensionless time is defined at $t^* = vt/H^2$, for $v = 4.806 \times 10^{-6}\ \text{m}^2\,\text{s}^{-1}$ and $H = 0.177$ m. The use of different time steps for each phase is similar to that in ref. [3] and it enables a precise resolution of the temperature distribution within the solid phase in which the effects of the transient terms are more significant than in the liquid phase.

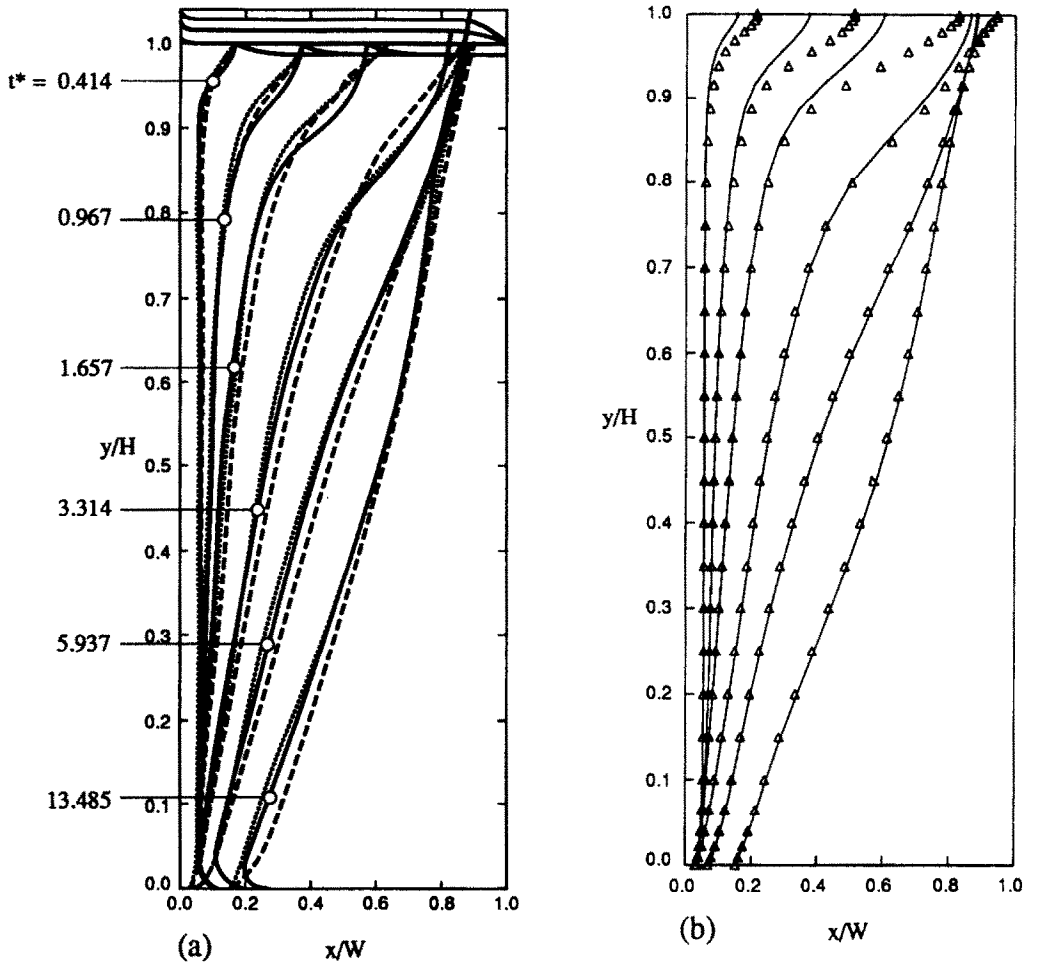

FIG. 5. The transient positions of the interface at various elapsed times. (a) Experimental (solid lines) and numerical (dashed lines) results from ref. [3] and numerical results from this study (dotted lines). (b) Present numerical results for the adiabatic case (solid lines) and the saturation temperature case (symbols).

3.3. *Results*

Numerical results are presented graphically as the positions of the interface at various elapsed times. This selection is made because the interface positions are gradient-controlled, and are thus the most diagnostic of the simulation (as compared to the distribution of the temperature- and velocity-fields). Figure 5(a) shows the numerical results for the interface position at various elapsed times for $0 \leqslant y/H \leqslant 1$. The experimental and numerical results from ref. [3] are also shown for comparison. In general, our numerical results agree well with the experiment in the lower part of the interface, while there is less agreement in the upper part. The same trend is also found in the numerical results of ref. [3]. Benard *et al.* [3] have claimed that the disagreement between their experimental and numerical results is due to the neglected non-orthogonal terms. However, we note that our method accounts for these terms, yet the local disagreement remains. Compared with the numerical results of ref. [3], the present method predicts slower movement of the interface. This is expected to be mainly due to the inclusion of non-orthogonal terms. The density difference and the liquid overflow slightly reduce the melting capacity of the liquid phase, but their influence on the movement of the interface is relatively small.

As was mentioned, the volume change causes the melt to flow over the solid phase through the outlet. Therefore, the boundary condition at the top surface of the solid phase varies with time, initially being that of nearly no heat flow across this surface (due to the presence of the air gap), and then that maintained nearly at the saturation temperature (due to the flow of the liquid over the solid). Also, the shape of this initially horizontal surface is continuously changing due to the fact that the flow of liquid over the solid phase results in heat transfer to the subcooled solid and, as a result, phase-change occurs at that surface. Therefore, the adiabatic thermal boundary condition assumed at the top surface of the solid phase, i.e. $\partial T_2/\partial y = 0$ in equation (29), is no longer valid. This

boundary condition should be modified in order to accurately predict the experimental results. To do this with a reasonable effort, the adiabatic condition is changed to the constant saturation-temperature condition, i.e. $T_2 = \hat{T}_1$ (with other boundary conditions unchanged). This boundary condition is also suggested and used in ref. [3]. The present numerical results obtained by using this modified boundary condition are shown in Fig. 5(b), where those obtained by using the adiabatic boundary condition are also redrawn for comparison. Note that the change in the boundary condition has a negligible effect on the interfacial motion in the lower part. However, in the upper portion of the enclosure, the interface moves substantially faster than that of the adiabatic boundary condition. Near the upper portion of the interface, the modified boundary condition causes the temperature gradients (normal to the interface) of the solid-phase to decrease significantly compared with those of the adiabatic boundary condition. Then, this locally reduced temperature gradient results in an increase in the melting rate of the solid (through the interfacial energy balance). This increased melting rate accelerates the local movement of the interface, as is evident in our numerical results given in Fig. 5(b), but we note that the numerical simulations of ref. [3] show no difference in the predicted interfacial locations, where both of the above-mentioned boundary conditions are used. This discrepancy will remain unsolved until more information becomes available on the implementations in ref. [3].

The present results suggest that neither of the two boundary conditions (adiabatic and saturation-temperature) at the top surface of the solid phase correctly simulates the experimental boundary condition there. The local disagreements with the experiment are expected to arise from the assumptions of the two-dimensionality of the system and the laminar flow regime, the neglected liquid-overflow above the solid phase and the use of the constant physical properties in the simulation.

4. SUMMARY

A numerical method is developed that is applicable to both diffusion- and convection/diffusion-controlled moving interface problems and accounts for the density difference between phases. A general coordinate transformation is employed to immobilize the moving interfaces. The resulting transformed equation is expressed in a conservative form and reflects the conservation principles in a moving, curvilinear control-volume in the physical coordinate. Therefore, even when the physical quantities such as density, velocity, enthalpy and transport properties change discontinuously across a given moving interface, the interface conditions become no more than the natural boundary conditions. This is because the components of the fluxes in the transformed equation are continuous across that interface. Moreover, since the transformed equation is developed only for a representative physical domain, a system made of a multiple number of moving interfaces can be treated without any further effort.

In deriving the finite-difference equations, the transformed governing equation is first integrated over the stationary control-volume in the transformed coordinate, and those integrated terms are then interpreted physically and discretized using the moving control-volume in the physical coordinate. For example, the pseudo-velocities arising from the immobilization of the moving interfaces are discretized according to the geometrical relation associated with the moving control-volumes. This special treatment of the pseudo-velocities has two major advantages. First, the pseudo-velocity fields independently satisfy the mass continuity regardless of the existence of the physical velocity fields. Then, diffusion-controlled moving boundary problems can be resolved without any creation of the parasitical mass sources. Second, the cases in which the physical domain boundaries move in both coordinate directions can be easily treated. The momentum equations are solved by using the physical covariant velocity components as dependent variables. However, the general transformed equation employed in this study can also accommodate the stream function–vorticity formulation, because the present treatment of the pseudo-velocities is still applicable. In the grid system composed of moving control-volumes, the directions of the base-vectors for the covariant velocity components change in time and space. The time-wise rotation of the velocity-component base-vectors is handled here by an algebraic manipulation, similar to the treatment of the spatial variation of those base-vectors suggested by others.

The method is applicable to two-dimensional problems with multiple, moving interfaces. Here, the solution method is tested against an example problem for which experimental results are available. For the combined convection and diffusion flux terms, the central-difference scheme is applied to the interfacial energy fluxes while the power-law scheme is used otherwise. The numerical results agree well with the available experimental results.

REFERENCES

1. C.-J. Kim and M. Kaviany, A numerical method for phase-change problems, *Int. J. Heat Mass Transfer* **33,** 2721–2734 (1990).
2. E. M. Sparrow, S. V. Patankar and S. Ramadhyani, Analysis of melting in the presence of natural convection in the melt region, *J. Heat Transfer* **99,** 520–526 (1977).
3. C. Benard, D. Gobin and A. Zanoli, Moving boundary problem: heat conduction in the solid phase of a phase-change material during melting driven by natural convection in the liquid, *Int. J. Heat Mass Transfer* **29,** 1669–1681 (1986).
4. M. Lacroix, Computation of heat transfer during melting of a pure substance from an isothermal wall, *Numer. Heat Transfer* **15B,** 191–210 (1989).
5. S. V. Patankar, *Numerical Heat Transfer and Fluid Flow*. Hemisphere, Washington, DC (1980).

6. K. C. Karki and S. V. Patankar, Calculation procedure for viscous incompressible flows in complex geometries, *Numer. Heat Transfer* **14**, 295–307 (1988).
7. E. M. Sparrow and W. Chuck, An implicit/explicit numerical solution scheme for phase-change problems, *Numer. Heat Transfer* **7**, 1–15 (1984).
8. K. C. Karki, A calculation procedure for viscous flows at all speeds in complex geometries, Ph.D. Thesis, University of Minnesota, Minneapolis (1986).

APPENDIX

The expressions for M_ξ^0, M_η^0, M_ξ and M_η, which were used in the discretization equation (13) for the velocity component $u_{\xi,e}$, are

$$M_\xi^0 = \left(\frac{h_{\xi,e}^0}{h_{\xi,e}}\right)\frac{x_{\xi,e}y_{\eta,e}^0 - y_{\xi,e}x_{\eta,e}^0}{J_e^0} - 1$$

$$M_\eta^0 = \left(\frac{h_{\eta,e}^0}{h_{\xi,e}}\right)\frac{y_{\xi,e}x_{\xi,e}^0 - x_{\xi,e}y_{\xi,e}^0}{J_e^0}$$

$$M_\xi = \left(\frac{h_\xi}{h_{\xi,e}}\right)\frac{x_{\xi,e}y_\eta - y_{\xi,e}x_\eta}{J} - 1$$

$$M_\eta = \left(\frac{h_\eta}{h_{\xi,e}}\right)\frac{y_{\xi,e}x_\xi - x_{\xi,e}y_\xi}{J}$$

where M_ξ and M_η are evaluated at the eight neighboring points (ee, w, Ne, Se, nE, sE, n and s in Fig. 1) and where M_ξ^0 and M_η^0 are evaluated only for the point e.

Similarly, the expressions for N_ξ^0, N_η^0, N_ξ and N_η for the velocity component $u_{\eta,n}$ are

$$N_\xi^0 = \left(\frac{h_{\xi,n}^0}{h_{\eta,n}}\right)\frac{x_{\eta,n}y_{\eta,n}^0 - y_{\eta,n}x_{\eta,n}^0}{J_n^0}$$

$$N_\eta^0 = \left(\frac{h_{\eta,n}^0}{h_{\eta,n}}\right)\frac{y_{\eta,n}x_{\eta,n}^0 - x_{\eta,n}y_{\xi,n}^0}{J_n^0} - 1$$

$$N_\xi = \left(\frac{h_\xi}{h_{\eta,n}}\right)\frac{x_{\eta,n}y_\eta - y_{\eta,n}x_\eta}{J}$$

$$N_\eta = \left(\frac{h_\eta}{h_{\eta,n}}\right)\frac{y_{\eta,n}x_\xi - x_{\eta,n}y_\xi}{J} - 1$$

where N_ξ and N_η are also evaluated at the eight neighboring points (nE, nW, nn, s, Ne, e, Nw and w in Fig. 1) and where N_ξ^0 and N_η^0 are evaluated only for the point n.

UNE METHODE NUMERIQUE POUR LES PROBLEMES DE CHANGEMENT DE PHASE AVEC CONVECTION ET DIFFUSION

Résumé—Une formulation existante aux différences finies qui utilise l'immobilisation de l'interface, pendant la préservation de la forme conservative des équations, est étendue pour inclure la convection et le changement de volume. Dans ce traitement bidimensionnel, les frontières physiques se déplacent dans les deux directions. Cela est permis par une technique nouvelle qui discrétise les pseudo-vitesses (du fait de l'immobilisation) en accord avec la relation géométrique associée aux volumes de contrôle mobiles. Les champs des pseudo-vitesses satisfont indépendamment la continuité de masse. Cela rend la méthode numérique adaptée aux problèmes de frontière mobile avec diffusion et diffusion convection. Dans la résolution des équations de quantité de mouvement, les composantes covariantes de vitesse sont choisies comme variables dépendantes et l'algorithme SIMPLER est utilisé pour le couplage entre les équations de continuité et de quantité de mouvement. La méthode est applicable aux problèmes avec plusieurs interfaces mobiles. En exemple, on considère une fusion dans une cavité bidimensionelle. Les prédictions sont comparées avec des résultats expérimentaux disponibles et on trouve un accord satisfaisant.

EIN NUMERISCHES VERFAHREN ZUR LÖSUNG VON PHASENWECHSELPROBLEMEN MIT KONVEKTION UND DIFFUSION

Zusammenfassung—Ein vorhandenes Finite-Differenzen-Modell, welches auf einer Festlegung der sich fortbewegenden Grenzfläche bei gleichzeitiger Beibehaltung der Erhaltungsgleichungen aufbaut, wird in der vorliegenden Arbeit erweitert um Konvektion und Volumenänderungen berücksichtigen zu können. In dem zweidimensionalen Modell ist es den physikalischen Berandungen möglich sich in beiden Koordinatenrichtungen zu bewegen. Dies wird mit Hilfe einer neuen Methode verwirklicht, bei der die Pseudogeschwindigkeiten (aufgrund der Festlegung) diskretisiert werden—abgestimmt auf die geometrische Situation und die sich bewegenden Kontrollvolumina. Dadurch befriedigen die Felder der Pseudogeschwindigkeit unabhängig die Massenerhaltung. Das vorgestellte numerische Verfahren kann somit auf Probleme mit beweglichen Berandungen angewandt werden, die entweder durch Diffusion oder durch Konvektion und Diffusion beeinflußt werden. Bei der Lösung der Impulstransportgleichung werden die physikalischen kovarianten Geschwindigkeitskomponenten als abhängige Variable gewählt. Für die Kopplung zwischen der Kontinuitätsgleichung und der Impulstransportgleichung wird der SIMPLER-Algorithmus verwendet. Diese Methode ist für Probleme mit mehreren sich bewegenden Grenzflächen verwendbar. Als anschauliches Beispiel wird der Schmelzvorgang in einem zweidimensionalen Hohlraum betrachtet. Die Rechenergebnisse werden abschließend mit verfügbaren Versuchsdaten verglichen, die Übereinstimmung ist gut.

ЧИСЛЕННЫЙ МЕТОД РЕШЕНИЯ ЗАДАЧ ФАЗОВОГО ПЕРЕХОДА ПРИ НАЛИЧИИ КОНВЕКЦИИ И ДИФФУЗИИ

Аннотация—Существующий метод конечных разностей, в котором используется фиксация движущейся границы раздела с сохранением консервативного вида уравнений, обобщается на случай учета конвекции и изменения объема. В предложенной двумерной формулировке предполагается движение физических границ в направлении обеих координат. С этой целью применяется новый метод, в котором псевдоскорость (возникающая за счет уменьшения подвижности) приводится к дискретному виду по геометрической зависимости, связанной с движущимися контрольными объемами. В результате поля псевдоскоростей самостоятельно удовлетворяют условию массовой непрерывности. Благодаря этому факту предложенный численный метод является пригодным для решения задач, в которых движение границы определяется диффузией, а также конвекцией и диффузией. При решении уравнений сохранения импульса предполагается, что физические компоненты ковариантной скорости являются зависимыми переменными и для сопряжения уравнений неразрывности и сохранения импульса используется алгоритм SIMPLER. Разработанный метод может применяться к задачам со множественными движущимися границами раздела. В качестве иллюстрирующего примера рассматривается процесс плавления в двумерной полости. Получено хорошее согласие между расчетными результатами и имеющимися экспериментальными данными.